New Method of Determination for Pressure and Shear Frictions in the Ring Rolling Process as Analytical Function

M.R. Zamani[*]

Mechanical Engineering Department, Sharif University of Technology, Iran, Tehran

ABSTRACT

Ring rolling is one of the most significant methods for producing rings with highly precise dimensions and superior qualities such as high strength uniformity, all accomplished without wasting any materials. In this article, we have achieved analytical formulas for calculating the pressure and shear friction over the contact arcs between the rollers and ring in the ring rolling process for the material in general nonlinear hardening property. We have also asserted the best mathematical model to predict friction for rolling processes. The method we use is based on calculating the analytical stress distribution. In other words, by using of Saint-Venan principal the stress components are calculated as analytical functions. Once that is accomplished, the pressure and shear traction over the rollers are able to be analyzed. The crucial characteristics which set apart this study from other studies are the investigation of the effects of the speed with which rollers are fed, and resulting ring velocity. With normal and shear friction, those characteristics cannot be investigated by other methods such as the slab method, upper bound, etc. Also, results show the effects of material hardening properties, radius of rollers and thickness reduction under pressure, and shear friction distributions.

© 2014 IAU, Arak Branch.All rights reserved.

Keywords: Ring rolling process; Analytical solution for pressure and shear tractions; Nonlinear material ; Friction model

1 INTRODUCTION

BECAUSE of the ring geometry, deformation gap, multi-motions of rollers, and many other intricate details involved in ring rolling, this process involves a high level of material nonlinearities and contact nonlinearities [1]. As the behavior of each of the materials and the parameters of the process in analyzing is very difficult, many researchers have not concerned all of these parameters in their analysis. The first experimental study of the ring rolling process was done by Johnson et al [2-3], and Hawkyard et al [4]. Yang and Kim [5] analyzed the ring rolling process with a finite element method for rigid-plastic material. They calculated the velocity field and external forces such as rolling force, rolling torque, and normal pressure distribution with results, and they validated their results using experimental methods.

By using of finite element method, Xu et al [6] investigated the effects of geometric parameters such as ring shape and curvature in regards to pressure distribution. In order to simulate the ring rolling process with a goal of calculating the pressure distribution, material spread, and rolling force numerically, Youngsoo et al [7] developed the finite element code SHAPE-PPTM. Theocarsis et al [8] like Yang and Kim used the optical acoustic reflection

_____
[*] Corresponding author. Tel.: +98 9306994332.
  E-mail address: mrzamani@alum.sharif.edu (M.R. Zamani).

method to investigate the normal pressure and shear traction over the contact surfaces within the rollers and ring. They too compromised their results with experimental methods. By using of a finite element code, ABAQUS, Wang et al [9] studied the influences of roll speed on the plate rolling process for investigating the normal pressure, Von-Misses stress, and rolling force. Additionally, they indicated that increasing the speed of the rollers rotation (ring velocity in exit zone) helps to decrease pressure and rolling force. By taking into account all of the studies which have been done to determine the pressure distribution in the ring rolling, many methods, such as the Slab Method and the Finite element to name a few, have been widely used. While some of these methods have advantages, they still can't claim a comprehensive report of pressure and shear friction in the ring rolling process. This includes all the significant parameters of rolling such as the speed of the roller feed, and rotating velocity or ring velocity in the exit, especially as analytical functions.

In this paper, we have calculated the pressure and shear friction over the contact arcs (surfaces) between the rollers and ring as analytical functions. In summary, by using the Saint-Venan Principal and understanding that the principal axes of strain rate are co-axial with the principal axes of stress, we have predicted the distribution of stress components as analytical functions throughout the deformation zone. Next, by using the stress transformation equations, we have calculated the pressure and shear friction as analytical functions in regards to rolling parameters such as rollers' radiuses, speed of the feed of rollers, ring velocity in the exit zone (rotating speed of rollers), varying ring thickness, and various material hardening properties.

2   MATHEMATICAL MODELS

As it is depicted in Fig.1, the ring rolling process includes two rollers which are much harder than the ring, so that the deformation or deflection of rollers can be neglected against ring deformation. While the rollers rotate around their axes, the force of the friction between the rollers and ring compels the ring to move forward. As the ring is pulling into the deformation zone; the rollers move toward each other. Therefore, the ring thickness is continuously reduced while its diameter continuously increases.
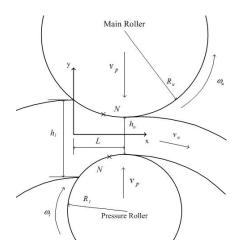

Fig. 1
Ring rolling's deformation zone.

As it was demonstrated by earlier researchers, the ring velocity in the entry zone is lower than the tangential velocity of rollers; in contrast, the ring velocity in the exit zone is more than the tangential velocity of rollers. For this reason, there should be a point along the contact length where the ring velocity and tangential velocity of rollers are equal together, and it is called the neutral point. Actually, the neutral point divides the deformation zone into two different zones i.e. entry zone and exit zone.

As far as the plastic strain in the material processing, especially in the ring rolling is much larger than the elastic strain, it is possible to ignore the elastic strain without any error [10]. When elastic strain is withdrawn, the principal stress axes will coincide with the principal axes of the strain rate or plastic strain [11]. By attention to this theory, we can write [11]

$$\tan(2\gamma) = \tan(2\gamma'), \tag{1}$$

In the above equation, γ is the principal axes of stress and γ' is the principal axes of strain rate over the deformation zone. They are calculated as [12]

$$\tan(2\gamma) = \frac{2\tau_{xy}}{\sigma_x - \sigma_y}, \qquad \tan(2\gamma') = \frac{2\dot{\varepsilon}_{xy}}{\dot{\varepsilon}_x - \dot{\varepsilon}_y}, \tag{2}$$

where σ_x, σ_y and τ_{xy} are normal and shear stress components in plane of deformation, as well as $\dot{\varepsilon}_x, \dot{\varepsilon}_y$ and $\dot{\varepsilon}_{xy}$ are normal and shear strain rate components in plane of deformation. Strain rate components originate from the velocity field, as below

$$\dot{\varepsilon}_x = \frac{\partial v_x}{\partial x}, \qquad \dot{\varepsilon}_y = \frac{\partial v_y}{\partial y}, \qquad \dot{\varepsilon}_{xy} = \frac{1}{2}\dot{\gamma}_{xy} = \frac{1}{2}\left(\frac{\partial v_x}{\partial y} + \frac{\partial v_y}{\partial x}\right). \tag{3}$$

where the v_x and v_y are the velocity components in direction of x and y, respectively. Since we considered the process plane strain, thus another component of velocity, stress and strain rate will be zero except the normal stress σ_z which is perpendicular to deformation plane, $x-y$ plane. Besides that in plastic deformation, material is incompressible, so that Poisson Ratio is 0.5 [11]. By considering the plane strain condition and Flow Rule, one obtains [13]

$$\sigma_z = \frac{\sigma_x + \sigma_y}{2}. \tag{4}$$

Therefore, by using of Eq.(4), Von-Misses yield criterion will be presented as:

$$\left(\frac{\sigma_x - \sigma_y}{2}\right)^2 + \tau_{xy}^2 = \sigma_{eq}^2, \tag{5}$$

where σ_{eq} is the equivalent stress which is related to the subsequent yield stress as $\sigma_Y / \sqrt{3}$, and for material with nonlinear hardening it is equal to

$$\sigma_{eq} = \frac{K}{\sqrt{3}}\varepsilon_{eq}^n, \tag{6}$$

where K and n are the material hardening parameters, and ε_{eq} is the equivalent plastic strain at deformation zone which is expressed by the plastic strain component as [11]

$$\varepsilon_{eq} = \sqrt{\frac{2}{3}\left(\varepsilon_r^2 + \varepsilon_\theta^2\right)}, \tag{7}$$

where ε_r and ε_θ are the radial and tangential strain components, respectively. By rearranging and squiring of Eq.(5), one gets

$$\left| \frac{\sigma_x - \sigma_y}{2} \right| = \sqrt{\sigma_{eq}^2 - \tau_{xy}^2},$$ (8)

Now we assume that the tensile stress is positive and the compressive stress is negative. Because the ring throughout the deformation zone is under compression, then the normal stress σ_y is compressive, negative. In addition, the ring is constrained from up and down sides and unconstrained from right and left sides, hence it is reasonable to consider that the normal stress in y-direction is more than the normal stress in x-direction [10]. As a result, Eq. (8) can be considered as:

$$\frac{\sigma_x - \sigma_y}{2} = \sqrt{\sigma_{eq}^2 - \tau_{xy}^2},$$ (9)

Substitution Eq. (9) into the first equation of Eqs. (2), and then the results are put into Eq.(1), finally one has

$$\tan(2\gamma') = \frac{\tau_{xy}}{\sqrt{\sigma_{eq}^2 - \tau_{xy}^2}}.$$ (10)

The right hand of second equation of Eqs. (2) is obtained from the assumed admissible velocity field in the ring at the deformation zone, thus the left hand of Eq. (10) is known. By solving Eq. (10) for shear stress, τ_{xy}, it is obtained as:

$$\tau_{xy} = \mp \frac{\tan(2\gamma)\,\sigma_{eq}}{\sqrt{1 + \tan(2\gamma)^2}},$$ (11)

where the positive sign implies the entry zone or left-hand side of the neutral point and negative sign implies the exit zone or right-hand side of the neutral point. The equilibrium equation for each ring particle in x-direction can be written as [12],

$$\frac{\partial \sigma_x}{\partial x} + \frac{\partial \tau_{xy}}{\partial y} = 0.$$ (12)

Substitution Eq. (11) into Eq. (12), and taking partial differential respect to y, and taking integrant respect to x, one gets

$$\sigma_x = \pm \frac{\partial}{\partial y} \left(\int \frac{\tan(2\gamma)\,\sigma_{eq}}{\sqrt{1 + \tan(2\gamma)^2}} dx \right) + A(y).$$ (13)

where $A(y)$ is an unknown function which will later be calculated from the boundary conditions over the contact surfaces between the rollers and ring in the deformation zone. Substituting of Eq. (13) and Eq. (11) into Eq. (9), the stress in y-direction is determined easily

$$\sigma_y = \pm \frac{\partial}{\partial y} \left(\int \frac{\tan(2\gamma)\,\sigma_{eq}}{\sqrt{1 + \tan(2\gamma)^2}} dx \right) + A(y) - 2\sqrt{\sigma_{eq}^2 - \left(\frac{\tan(2\gamma)\,\sigma_{eq}}{\sqrt{1 + \tan(2\gamma)^2}} \right)^2}.$$ (14)
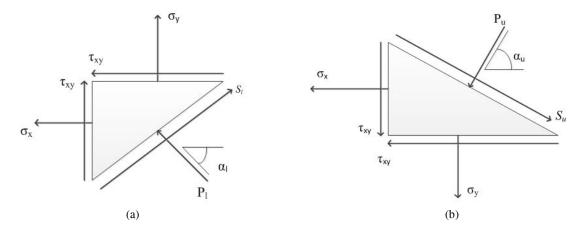
Fig. 2
Material elements near the surfaces of upper and lower rollers. a) lower element b) upper element

Fig. 2 shows the ring elements near the surfaces of the upper and lower rollers.

If one writes the stress transformation equations [14-15] for ring elements near the upper roller and lower roller, the pressure and shear friction distributions are obtained along the contact arcs within the ring and rollers. Therefore, for ring elements near the main roller surface:

$$P_u = \frac{\sigma_x + \sigma_y}{2} + \frac{\sigma_x - \sigma_y}{2}\cos(2\alpha_u) + \tau_{xy}\sin(2\alpha_u),$$

(15)

$$S_u = -\frac{\sigma_x - \sigma_y}{2}\sin(2\alpha_u) + \tau_{xy}\cos(2\alpha_u),$$

(16)

For ring elements near the pressure roller surface:

$$P_l = \frac{\sigma_x + \sigma_y}{2} + \frac{\sigma_x - \sigma_y}{2}\cos(2\alpha_l) + \tau_{xy}\sin(2\alpha_l),$$

(17)

$$S_l = -\frac{\sigma_x - \sigma_y}{2}\sin(2\alpha_l) + \tau_{xy}\cos(2\alpha_l).$$

(18)

In Eqs. (15) to (18), the α_u angle shows the ring particles' positions along the upper roller's surface, and it is measured based on a line which passes through the ring particles along the upper roller's surface and the center of the upper roller respect to the horizontal line, and α_l is defined similarly to α_u but for ring particles along the lower roller. By paying attention to Fig. 3, one can perceive $\alpha + \theta = \dfrac{\pi}{2}$, therefore the functions $\sin(2\alpha_u)$, $\sin(2\alpha_l)$, $\cos(2\alpha_u)$ and $\cos(2\alpha_l)$ are determined as:

$$\sin(2\alpha_u) = \sin(2\theta_u) = 2\frac{L-x}{R_u}\sqrt{1 - \left(\frac{L-x}{R_u}\right)^2},$$

(19)

$$\sin(2\alpha_l) = \sin(2\theta_l) = 2\frac{L-x}{R_l}\sqrt{1 - \left(\frac{L-x}{R_l}\right)^2},$$

(20)

$$\cos(2\alpha_u) = -\cos(2\theta_u) = 2\left(\frac{L-x}{R_u}\right)^2 - 1, \tag{21}$$

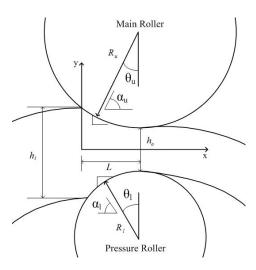$$\cos(2\alpha_l) = -\cos(2\theta_l) = 2\left(\frac{L-x}{R_l}\right)^2 - 1. \tag{22}$$

Fig. 3
Indication of the rolling's parameters in deformation zone.

In Eqs. (19) to (22), R_u stands for the main, upper, roller radius and R_l stands for the pressure, lower, roller radius. L stands for contact length between the ring and the rollers. The contact length is defined by [16]

$$L = \left[R_u^2 - \left(\frac{\left(R_u + R_l + h_i - h_o\right)^2 + R_u^2 - R_l^2}{2\left(R_u + R_l + h_i - h_o\right)} \right)^2 \right]^{\frac{1}{2}} \tag{23}$$

By neglecting of elastic slip zone in the entry and recovery elastic of ring in the exit zone, little before the first point of the contact length and little after the last point of the contact length, the pressure between rollers and ring at these points is zero. Therefore, the boundary conditions for determining of $A(y)$ obtained as below

$$P_u\,|_{x=0-\delta} = 0, \qquad P_l\,|_{x=0-\delta} = 0, \tag{24}$$

$$P_u\,|_{x=L+\delta} = 0, \qquad P_l\,|_{x=L+\delta} = 0, \tag{25}$$

$$S_u\,|_{x=0-\delta} = 0, \qquad S_l\,|_{x=0-\delta} = 0, \tag{26}$$

$$S_u\,|_{x=L+\delta} = 0, \qquad S_l\,|_{x=L+\delta} = 0, \tag{27}$$

Eqs. (24) and (26) determine the function $A(y)$ for entry zone and Eqs. (25) and (27) determine the function $A(y)$ for exit zone. It is worthy to be noticed, since function $A(y)$ is function of height, independent on contact length, by having function $A(y)$ in one section along the contact length we can develop it for rest of the entry or exit regions. Eqs. (24) to (27) express eight conditions for function $A(y)$ or four conditions for each zone, thus the function $A(y)$ is offered as a third order equation, as below, and its coefficients are determined by Eqs. (24) to (27)

$$A_{entry}(y) = a_0 + a_1 y + a_2 y^2 + a_3 y^3, \tag{28}$$

$$A_{exit}(y) = a_0' + a_1' y + a_2' y^2 + a_3' y^3, \tag{29}$$

Finally, the normal pressure and the shear friction distributions over the rollers are determined as below

$$P_u = \frac{\partial}{\partial y}\left(\int \frac{\tan(2\gamma)\,\sigma_{eq}}{\sqrt{1+\tan(2\gamma)^2}}dx \right) + A_{entry}(y) - \sqrt{\sigma_{eq}^2 - \left(\frac{\tan(2\gamma)\,\sigma_{eq}}{\sqrt{1+\tan(2\gamma)^2}} \right)^2} +$$

$$\sqrt{\sigma_{eq}^2 - \left(\frac{\tan(2\gamma)\,\sigma_{eq}}{\sqrt{1+\tan(2\gamma)^2}} \right)^2}\left(1 - 2\left(\frac{L-x}{R_u} \right)^2 \right) + 2\frac{\tan(2\gamma)\,\sigma_{eq}}{\sqrt{1+\tan(2\gamma)^2}}\frac{L-x}{R_u}\sqrt{1-\left(\frac{L-x}{R_u} \right)^2}, \tag{30}$$

$$S_u = -\sqrt{\sigma_{eq}^2 - \left(\frac{\tan(2\gamma)\,\sigma_{eq}}{\sqrt{1+\tan(2\gamma)^2}} \right)^2}\left(2\frac{L-x}{R_u}\sqrt{1-\left(\frac{L-x}{R_u} \right)^2} \right) + \left(\frac{\tan(2\gamma)\,\sigma_{eq}}{\sqrt{1+\tan(2\gamma)^2}} \right)\left(1 - 2\left(\frac{L-x}{R_u} \right)^2 \right), \tag{31}$$

For entry zone; and for exit zone

$$P_u = -\frac{\partial}{\partial y}\left(\int \frac{\tan(2\gamma)\,\sigma_{eq}}{\sqrt{1+\tan(2\gamma)^2}}dx \right) + A_{exit}(y) - \sqrt{\sigma_{eq}^2 - \left(\frac{\tan(2\gamma)\,\sigma_{eq}}{\sqrt{1+\tan(2\gamma)^2}} \right)^2} +$$

$$\sqrt{\sigma_{eq}^2 - \left(\frac{\tan(2\gamma)\,\sigma_{eq}}{\sqrt{1+\tan(2\gamma)^2}} \right)^2}\left(1 - 2\left(\frac{L-x}{R_u} \right)^2 \right) - 2\frac{\tan(2\gamma)\,\sigma_{eq}}{\sqrt{1+\tan(2\gamma)^2}}\frac{L-x}{R_u}\sqrt{1-\left(\frac{L-x}{R_u} \right)^2}, \tag{32}$$

$$S_u = -\sqrt{\sigma_{eq}^2 - \left(\frac{\tan(2\gamma)\,\sigma_{eq}}{\sqrt{1+\tan(2\gamma)^2}} \right)^2}\left(2\frac{L-x}{R_u}\sqrt{1-\left(\frac{L-x}{R_u} \right)^2} \right) - \left(\frac{\tan(2\gamma)\,\sigma_{eq}}{\sqrt{1+\tan(2\gamma)^2}} \right)\left(1 - 2\left(\frac{L-x}{R_u} \right)^2 \right), \tag{33}$$

In order to plot the normal pressure distribution over the rollers' surface, the Eqs. (30) and (32) should be plotted in one figure why their intersection shows the position of the neutral point.

3   RESULTS

Here, we plot the pressure and the shear friction over the contact length between the rollers and ring for different values of the rollers' radius, the ring velocity in the exit section and the speed of the rollers feed for different materials. By attention to behaviors of shear friction, finally, we demonstrate the best approximate for prediction of the shear friction in the ring rolling process. In order to calculate the direction of principal axes of the strain rate in the deformation zone, we used the velocity field that is provided by [17]

$$v_x = -\int_{L_n}^{x} \frac{v_p}{2g(\zeta)} d\zeta + \frac{v_o h_o}{2g(x)}, \tag{34}$$

$$v_y = \frac{h_o v_o}{2g^2(x)} \frac{\partial g(x)}{\partial x} y + \frac{h_o v_o}{2g^2(x)} \left\{ \frac{\partial h(x)}{\partial x} g(x) - \frac{\partial g(x)}{\partial x} h(x) \right\} + v_p \frac{y - h(x)}{2g(x)}, \tag{35}$$

where v_o stands the ring velocity in the exit section, and v_p stands the speed of the rollers feed, also $h(x)$ and $g(x)$ are the height of the deformation zone and amounts of the distinct between the situation of the roll gap and the x-axis in the deformation zone which are defined according [17], respectively. v_x stands velocity of particles in x-direction and v_y stands velocity of particles in y-direction.

In Fig.4, we plotted the pressure distribution over the contact length between the upper roller and ring. According to [14], by increasing of thickness reduction- the reduction correlates with the speed of the feed directly-the pressure is increased, the pressure peak is in the neutral point- actually; in all Figs. 4 to 8 the maximum points show the neutral points' positions. The position of the neutral point moves toward the entrance section while the ring thickness is reduced in the exit section. Moving of the neutral point toward the entrance section is inappropriate, because the effective area which leads to the ring being transmitted into the deformation zone reduces until the process stops. As the rollers' radius is increased, the maximum value of the pressure is increased. As a result from Fig.4 and Fig.5, for rolling of thin ring we should use rollers with lower radius when reduction is high.

It was explained by [18] that increasing of the ring velocity in the exit section or the rollers' rotating velocity leads the stress components distribution in the deformation zone to reduce. Therefore, the pressure distribution is decreased by increasing of the ring's velocity in the exit section as depicted in Fig.6, and the position of the neutral point moves toward the exit section, which is very suitable for the rolling process.
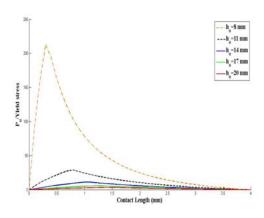

Fig. 4
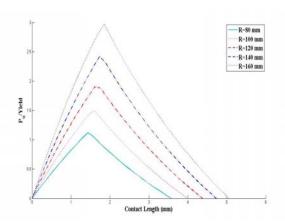The Pressure Distribution over the contact length.

Fig. 5
Rollers radius effects on the pressure distribution.

In contrast, increasing of the speed of the feed causes the pressure distribution to increase. Thus, there should be a relationship between the speed of the feed and the ring's velocity in the exit section for optimization of the pressure distribution over the contact length.
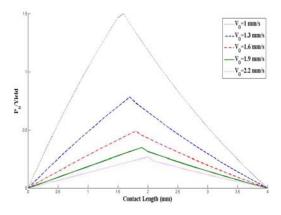

Fig. 6
Effects of the ring velocity in the exit section on the pressure distribution.
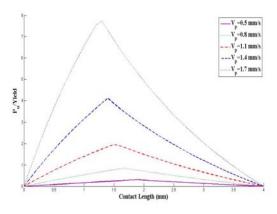

Fig. 7
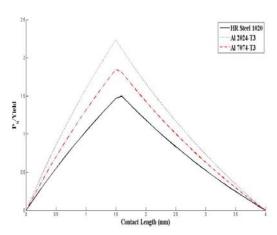Variation of pressure distribution by speed of rollers' feed.

Fig. 8
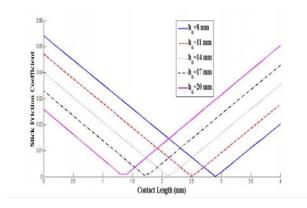Effects of the materials' properties on the pressure distribution.

Fig. 9
Stick Friction Coefficient for different ring thickness.
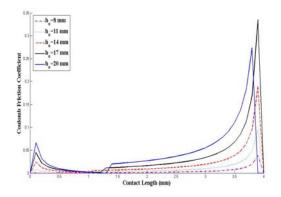
Fig. 10
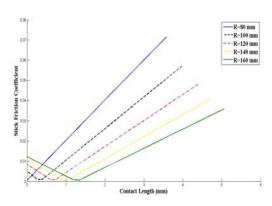Coulomb Friction Coefficient for different ring thickness.

Fig. 11
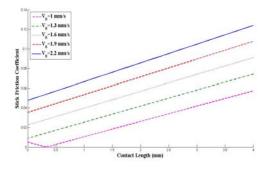Effects of rollers radius on stick friction coefficient.

Fig. 12
Stick Friction Coefficient for different values of ring velocity in the exit section.
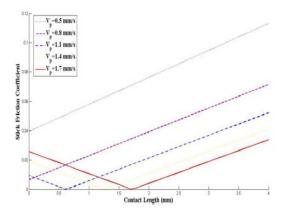
Fig. 13
Stick Friction Coefficient for different values of the speed
of the rollers' feed.

In Figs. 9 to 13, we have depicted the stick and coulomb friction coefficients over the contact length between the rollers and ring for different parameters of the process. The stick friction coefficient is defined by dividing the shear stress over the contact length to the equivalent yield stress of material, which is defined as [14]

$$\sigma_{eq} = \frac{K}{n+1} \varepsilon_{eq}^{n},$$ (36)

The coulomb friction coefficient is defined by dividing the shear stress throughout the contact length to the pressure distribution throughout the contact length. Since the pressure and shear distributions near the entrance and exit sections converge to zero, the coulomb friction in these sections increases to an unlimited degree, undefined. Hence, to show the details of friction coefficient variations, we refused to plot friction coefficients for these sections. In all of the figures, the friction coefficient has its minimum values at the neutral point- actually; in all Figs. 9 to 13 the minimum points show the neutral points' positions. By paying attention to variations of friction coefficient or shear stress, it can be concluded that the best model for demonstrating the shear stress is a function of the velocity of slip as below

$$S_u = G(v_x - v).$$ (37)

Since moving from the entrance section toward the neutral point, the difference between the ring particles' velocity near the rollers surfaces reduces (in the neutral point is assumed the ring particles' velocity is equal to the rollers tangential velocity), and after that the difference between them increases. Thus, it can be determined that the shear stress is proportionate to slip velocity, as it was presented to be [19]

$$S_u = \mu \frac{v_x - v}{T},$$ (38)

where μ is friction coefficient, v tangential velocity of rollers and T is oil film thickness, according to [19].

4   CONCLUSIONS

In a nutshell, we have presented a new method for calculating the pressure and shear stress distributions over the contact length as analytical functions in the Ring Rolling Process. The most significant aspect of this method is the investigation of effects of the ring velocity in the exit section (rotational velocity of rollers), the speed of the rollers feed, etc., on the pressure and shear stress distributions as analytical functions. This is something that cannot be achieved by other methods such as the slab or upper bound methods, to name a few. We have already illustrated the

pressure distribution for different rolling process parameters, and it is shown that the lower values of ring thickness in the exit section, the higher the values of the speed of rollers feed, and the higher values of rollers' radius all have detrimental effects on the pressure distribution. In contrast, the higher values of ring velocity in the exit section (rotational velocity of rollers) have suitable effects on the pressure distribution. In addition, we illustrated the shear stress distribution for different parameters of rolling, as well as drawing attention to shear stress figures, we suggested that the best model for predicting behaviors of shear stress should be a function of slip velocity between ring and rollers' surfaces.

REFERENCES

[1]   Zhang Xu., Wan Qi., Zhigang Li., 2011, Solver for finite element analysis of ring rolling process, *Advanced Materials Research* **338**: 251-254.

[2]   Johnson W., MacLeod I., Needham G., 1968, An experimental investigation into the process of ring or metal tyre rolling, *International Journal of Mechanical Sciences* **10**: 455-476.

[3]   Johnson W., Needham G., 1968, Experiments on ring rolling, *International Journal of Mechanical Sciences* **10**: 95-113.

[4]   Hawkyard J. B., Johnson W., Kirkland J., Appleton E., 1973, Analyses for roll force and torque in ring rolling, with some supporting experiments, *International Journal of Mechanical Sciences* **15**: 873-893.

[5]   Yang D. Y., Kim K. H., 1988, Rigid-plastic finite element analysis of plane strain ring rolling, *International Journal of Mechanical Sciences* **30**: 571-580.

[6]   Xu S.G., Lian J.C., Hawkyard J.B., 1991, Simulation of ring rolling using a rigid-plastic finite element model, *International Journal of Mechanical Sciences* **33**: 393-401.

[7]   Youngsoo Y., Youngsoo K., Naksoo K., Jongchan L., 2003, Prediction of spread, pressure distribution and roll force in ring rolling process using rigid-plastic finite element method, *Journal of Materials Processing Technology* **140**: 478-486.

[8]   Theocaris P. S., Stassinakis C. A., Mamalis A. G., 1983, Roll-Pressure distribution and coefficient of friction in hot rolling by caustics, *International Journal of Mechanical Sciences* **25**: 833-844.

[9]   Wang B., Hu W., Kong L.X., Hodgson P., 1998, The influence of roll speed on the rolling of metal plates, *Metals and Materials* **4**: 915-919.

[10]   Hill R., 1950, *The Mathematical Theory of Plasticity*, Published in the United States by Oxford University Press Inc. New York, First Published.

[11]   Akhtar S.K., Surjian H., 1995, *Continuum Theory of Plasticity*, Wiley-Interscience Pulication, John Wiley and Sons, Inc.

[12]   Barber JR., 1992, *Elasticity*, Kluwer, Dordrecht, The Netherlands, Second Edition.

[13]   Salimi M., Kadkhodaei M., 2004, Slab analysis of asymmetrical sheet rolling, *Journal of Materials Processing Technology* **150**: 215-222.

[14]   Hossford W.F., Caddel R.M., 2011, *Metal Forming Mechanics & Metallurgy*, Cambridge University Press fourth Edition.

[15]   Salimi M., Sassani F., 2002, Modified slab analysis of asymmetrical plate rolling, *International Journal of Mechanics Science* **44**: 1999-2023.

[16]   Ryoo J.S., Yang D.Y., 1986, The influence of process parameters on torque and load in ring rolling, *Journal of Mechanical Working Technology* **12**: 307-321.

[17]   Ryoo S., Yang D.Y., Johnson W., 1983, Ring rolling; the inclusion of pressure roll speed for estimating torque by using a velocity superposition method, *Proceedings of 24th International MTDR Conference* ,Manchester.

[18]   Wang B., Hu W., Kong L.X., Hodgson P., 1998, The influence of roll speed on the rolling of metal plates, *Metal and Materials* **4**(4): 915-919.

[19]   Ginzburg B.V., Ballas R., 2002, *Fundamentals of Flat Rolling Manufacturing Engineering and Materials Processing*, Published by CRC Press.